SAND2014-15431C

Critical detonation thickness in vapor-deposited hexanitroazobenzene (HNAB) films with different preparation conditions

Alexander S. Tappan, Ryan R. Wixom, and Robert Knepper

Explosives Technologies Group
Sandia National Laboratories, Albuquerque, NM 87185

Abstract. Hexanitroazobenzene (HNAB) films were deposited on polycarbonate through physical vapor deposition. HNAB deposits as an amorphous film that subsequently crystallizes over time. The temperature under which this crystallization occurs affects the microstructure of the HNAB and the resulting detonation properties. By varying the crystallization conditions experienced by vapor deposited amorphous HNAB, changes in microstructure arise that affect near failure detonation behavior. Specifically, HNAB crystallized at room temperature has uniformly distributed pores with diameters generally less than 150 nm and has a critical thickness of 63.4 ± 1.3 μm. Elevated temperature crystallization results in less-well distributed porosity and larger detonation failure thicknesses.

Introduction

At Sandia National Laboratories, we have coined the term "microenergetics" to describe sub-millimeter energetic material studies aimed at gaining knowledge of combustion and detonation behavior at the mesoscale. Characteristics of the microstructure, especially porosity, dramatically influence explosive behavior such as initiation, growth to detonation, and detonation failure. These effects on continuum behavior have been shown through experiments on detonation failure with different particle sizes or specific surface area of explosives (e.g., work on 3,4-dinitrofurazanfuroxan (DNTF) and 2,4,6,8,10,12-hexanitro-2,4,6,8,10,12-hexaazaisowurtzitane (CL-20)),[1] as well as experiments on homogeneous explosives with added heterogeneities (e.g., nitromethane-nitroethane/glass microballoons).[2] Mesoscale and microscale behavior such as the lateral structure at the detonation front,[3] as well as the overall rate of chemical energy release across the length of the reaction zone are assumed to also arise from these microstructural features.

Previous work on vapor-deposited explosives has been conducted with PETN (pentaerythritol tetranitrate) utilizing Sandia's critical thickness experiment.[4, 5] This experiment presents a two-dimensional analogue (critical thickness) to the more typical one-dimensional rate stick experiment (critical diameter). Initial work introduced the experiment and geometrical effects of deposited film width (in the plane of the fused silica substrate) on failure,[4] with later work presenting the effect of PETN deposition conditions.[5] We are currently applying physical

vapor deposition of explosives to examine the effects of confinement on detonation behavior,[6] as well as the effects of microstructure arising from deposition conditions on detonation. Through this work we hope to inform mesoscale modeling efforts that have traditionally relied on inferences from large-scale experiments.

The present work applies the critical thickness detonation experiment to vapor-deposited HNAB (hexanitroazobenzene) prepared under different crystallization conditions. HNAB deposits as an amorphous film that subsequently crystallizes over time.[7] We utilize this crystallization as a means to prepare samples with different microstructure characteristics to evaluate the effect on detonation properties. The temperature under which this crystallization occurs affects the porosity distribution of the HNAB and the resulting detonation properties, such as critical thickness.

Experimental

HNAB samples are prepared through physical vapor deposition on polycarbonate substrates in a custom deposition chamber. HNAB deposits as a fully dense amorphous film and crystallizes over time to a dense film (>99% dense) of principally HNAB-II with some proportion of an unknown crystal structure.[7] HNAB is deposited in two lines on 1.00 × 3.00 cm polycarbonate substrates, yielding two velocity data sets for each detonation experiment. Deposition thicknesses range from 50 µm to greater than 200 µm. Each line is 1.6 mm wide and therefore side losses during detonation are assumed to be insignificant with respect to losses associated with the thickness of the film.

After deposition, HNAB films are crystallized at temperatures ranging from ambient to 85 °C. At ambient conditions, the films complete crystallization typically within three to four weeks. At 65 °C the films crystallize within a few hours. Crystallization at 85 °C, above the glass transition temperature (~70 °C), appears to change the crystallization mechanism and results in films that are different in color and surface appearance than the other films.[7]

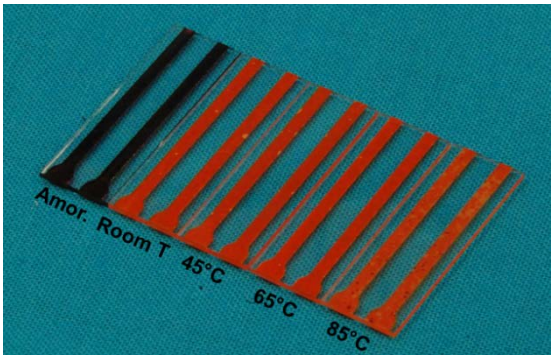

Figure 1. Photograph of HNAB films deposited on polycarbonate with different crystallization conditions. The leftmost film is as-deposited with increasing crystallization temperature to the right.

The characterization of the HNAB films after deposition and crystallization is conducted with optical microscopy, surface profilometry, and scanning electron microscopy. After crystallization, film thickness is measured in 13 locations along the lines corresponding to the positions and halfway points of the 7 optical fibers used for detonation velocity measurements (see below). Film thickness is reported as the average of the 13 average step heights across a 100 µm band approximately in the center of the film. Error is reported to be ± the standard deviation of this value. Ion polishing was conducted on some films using a JEOL IB-09010CP cross section polisher to reveal interior features of the microstructure in a similar fashion to the focused ion beam technique that has been used on other explosives.[8] Scanning electron microscopy was conducted on some films to examine surface features as well as interior microstructure.

Detonation velocity was determined using the aforementioned critical thickness experiment.[4] In this experiment, a PETN structure is used to ignite the two deposited HNAB lines. Passive optical fiber probes send light from each of the detonating explosive lines to photodetectors. Only experiments that yielded data spanning at least 4 of the optical fibers (10.5 mm) are used in the data analysis. A linear least squares fit is applied to the position versus time data from the photodetectors and error is reported as ± the standard error of this fit. In addition to the photodetector data, the

detonation is simultaneously recorded with a framing camera and a streak camera.

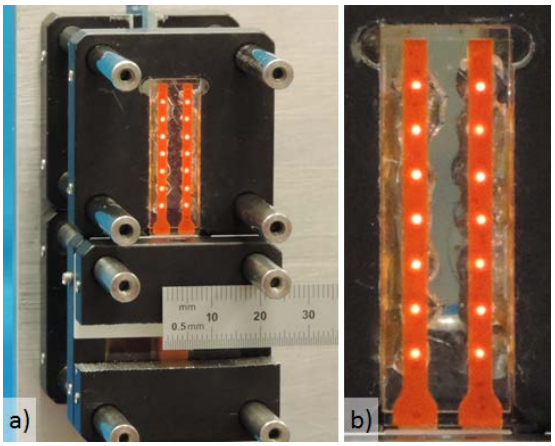

Figure 2. Photographs of Sandia's critical thickness experiment. a) The lower portion of the experiment contains the PETN ignition structure, and b) the upper portion of experiment contains the deposited HNAB lines and optical fiber probes (illuminated to show position).

Results

Numerous experiments were conducted on HNAB lines of different thicknesses that were crystallized at room temperature, 45 °C, and 65 °C. In addition, a few scoping experiments were conducted on as-deposited (amorphous) HNAB lines and HNAB lines that were crystallized at 85 °C, above the glass transition temperature of HNAB. HNAB lines of thicknesses up to ~140 µm at these two conditions did not detonate. Detonation in an HNAB sample with line thicknesses of 95 and 102 µm crystallized at 45 °C is shown in Figure 3.

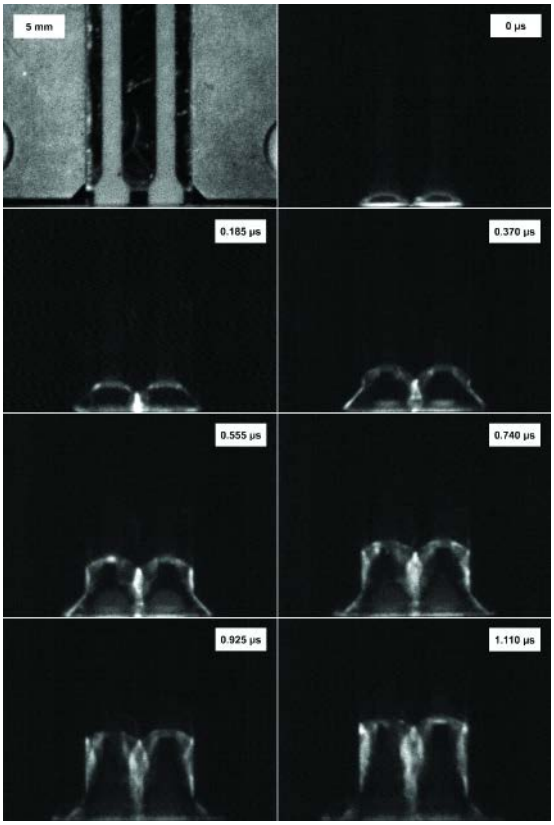

Figure 3. Framing camera images of detonation in the two lines of a single HNAB sample crystallized at 45 °C. These images were taken at 5.4 million frames-per-second (1/185 ns) with an exposure time of 15 ns.

Detonation in HNAB films crystallized at room temperature, 45 °C, and 65 °C was possible at thicknesses of ~100 µm and smaller depending on the crystallization conditions. The HNAB film thickness necessary to sustain a detonation increased as the crystallization temperature increased. Graphs of detonation velocity versus film thickness for HNAB crystallized at these three conditions are shown in Figure 4.

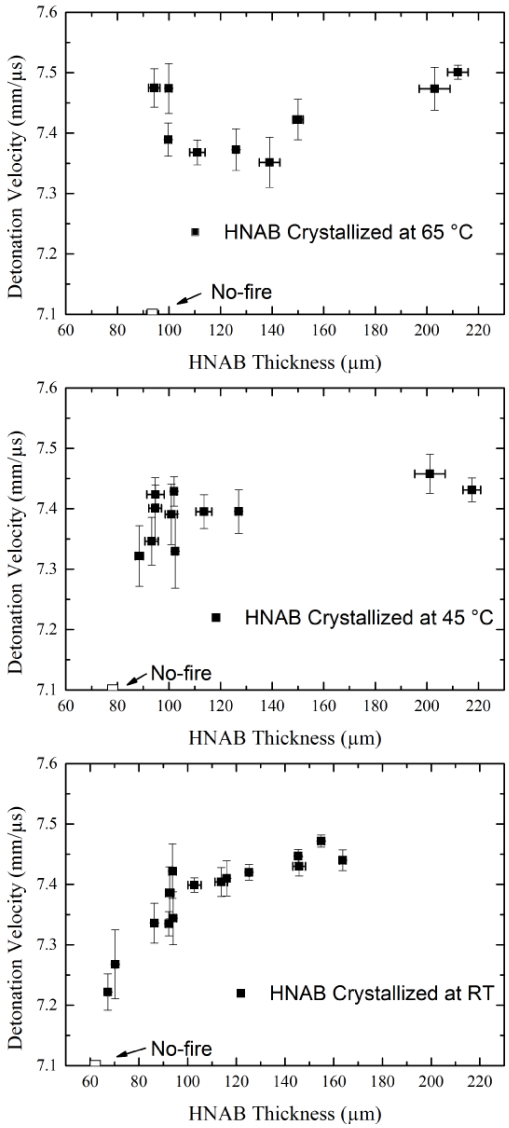

Figure 4. Detonation velocity versus HNAB thickness for HNAB crystallized at room temperature (RT, bottom), 45 °C (middle), and 65 °C (top). The open symbol represents the thickest films where detonation was consistently unable to propagate. Thicker no-fires are treated as no-tests due to the inability to measure a velocity and presumed initiation issues.

The detonation velocity measurements for HNAB crystallized at room temperature consist of 16 different line thicknesses, all that detonated except for the one open symbol shown in Figure 4 with a thickness of 62.1 ± 0.5 μm. Other thicknesses that did not detonate are not shown. The experimental failure thickness, t_f is defined as the average thickness of the fire and no-fire experiments nearest failure. The data show a monotonic decrease in detonation velocity with decreasing film thickness. Each detonation velocity calculated from the optical fiber probe data within this sample set has a relatively low uncertainty when compared to the data for HNAB crystallized at higher temperatures.

The detonation velocity measurements for HNAB crystallized at the two higher temperatures of 45 and 65 °C have distinct differences from those for HNAB crystallized at room temperature. The most obvious difference is the increased scatter in the data and the lack of a gradual decrease in detonation velocity approaching failure. This is especially true in the data for HNAB crystallized at 65 °C. Additionally, the error in any individual velocity measurement is greater than that for HNAB samples crystallized at room temperature.

Discussion

The differences in trends within the detonation velocity versus HNAB thickness plots shown in Figure 4 must arise from physical differences within the film as opposed to chemical differences. All as-deposited amorphous films are chemically identical with crystallization temperature being the only difference between them. There are qualitative differences between the crystallized films that can be observed in the surface profilometry measurements. In general, the incidence of surface defects and cracks increases with increasing crystallization temperature. It is reasonable that as crystallization time decreases at higher temperatures, there is less time for stress arising during the crystallization process to relax uniformly throughout the film. Thus, faster crystallization typically leads to larger defects and greater inconsistencies in the detonation behavior. However, these large scale defects, spanning hundreds of microns, are not the only effects arising from crystallizing at different temperatures.

The microstructure of HNAB crystallized at room temperature as examined using cross section

ion polishing and scanning electron microscopy reveals internal porosity (top of Figure 5). The HNAB has uniformly distributed pores with diameters generally less than 150 nm as shown in the histogram at the bottom of Figure 5. The distribution of these pores is uniform as contrasted with the porosity in HNAB crystallized at higher temperatures. In films crystallized at 45 and 65 °C, the internal porosity consists of fewer larger pores that have larger domains of non-porous HNAB between them. This difference in porosity distribution can have implications on detonation propagation. First, the more gradual decline in detonation velocity with decreasing thickness in the HNAB crystallized at room temperature could result from the distributed porosity where these heterogeneities become hot spots that support reaction as the films approach the failure thickness. Second, if the distribution is such that distances between adjacent pores exceeds typical length scales associated with the reaction zone length (< 1.2 μm)[6] then no coalescence of hot spots is possible to support reaction.

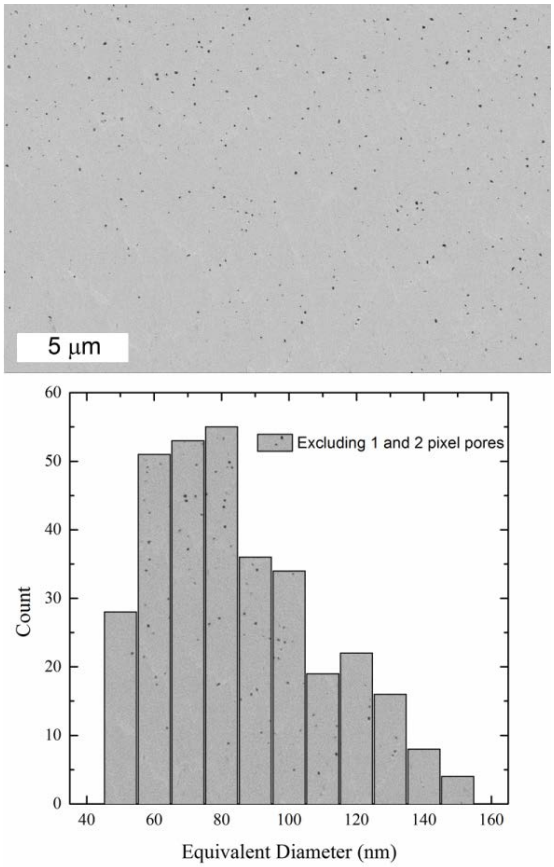

Figure 5. (top) Scanning electron micrograph of an ion-polished cross-section of HNAB crystallized at room temperature with distributed pores with diameters less than 150 nm as shown in the (bottom) histogram.

Critical thickness data were analyzed similarly to the technique used by Campbell and Engelke for critical diameter data.[9] Their form for diameter effect data can be applied to films of effectively infinite width by substituting radius with thickness.[2] Finally, the equation can be rewritten to facilitate fitting data in the detonation velocity versus inverse thickness plane:

$$D(R) = D(\infty)\left[1 - \frac{1}{t}\left(\frac{A}{1-t_c\frac{1}{t}}\right)\right], \qquad (1)$$

where *D(R)* is detonation velocity at a given explosive thickness (mm/μs), $D(\infty)$ is the detonation velocity at infinite radius (mm/μs), *A* is

a length parameter that describes the shape of the curve near failure (μm), t is the explosive thickness (μm), and t_c is a length parameter defined as critical thickness (μm). The experimental failure thickness, t_f is different than t_c, which represents a non-physical asymptote.

For the three different crystallization conditions, HNAB detonation velocity versus inverse thickness is shown in Figure 6. The single open symbol at the horizontal axis for each data set is the thickest no-fire point. For each of the three HNAB crystallization conditions, the detonation velocity asymptote at "infinite thickness" is essentially identical. Thus, for thick films, the characteristics of the HNAB and most importantly for this comparison, the density, is the same. The differences in the thickness asymptote at "critical thickness" is more pronounced, with increasing crystallization temperature leading to increasing critical thickness. Thus, the microstructure of the HNAB plays an important role in behavior near failure, likely generating hot spots to support reaction. Values for $D(\infty)$, A, and t_c are shown in Table 1.

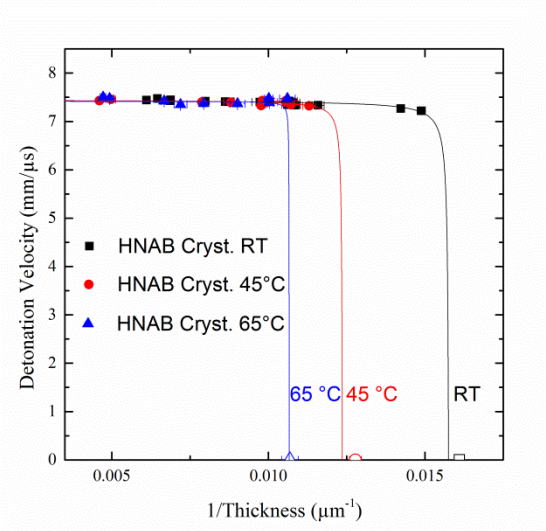

Figure 6. Critical thickness curves for HNAB crystallized at room temperature, 45 °C, and 65 °C. Analysis is conducted in the form of Campbell and Engelke.[9]

Table 1. Values for the three parameters derived from analysis of detonation versus inverse thickness for HNAB at three crystallization temperatures.

Crystallization Temperature	**Detonation Velocity at Infinite Thickness, D(∞) mm/μs**	**Critical Thickness, t_c μm**	**Length Parameter, A μm**
Room T	7.424 ± 0.012	63.4 ± 1.3	0.120 ± 0.043
45 °C	7.435 ± 0.020	80.8 ± 2.6	0.109 ± 0.053
65 °C	7.417 ± 0.061	93.8 ± 0.2	0.025 ± 0.016

Detonation was not achieved in as-deposited (amorphous) HNAB samples as thick as ~140 μm. Fracture cross sections of the amorphous films show that there is no observable porosity. This lack of porosity prevents hot spot formation during initiation and no reaction is supported within the HNAB. The amorphous HNAB represents an extreme condition in a solid explosive where there is absolutely no long-range order, crystallinity, or porosity. Through control of crystallization of this amorphous HNAB, it may be possible to gradually transition from homogeneous to heterogeneous explosive behavior in a solid explosive, allowing studies on initiation and growth to detonation.

Conclusions

We have shown that by varying the crystallization conditions experienced by vapor deposited amorphous HNAB, changes in microstructure arise that affect detonation behavior at near failure conditions. Specifically, we show that HNAB crystallized at room temperature has uniformly distributed pores with diameters generally less than 150 nm and has a critical thickness of 63.4 ± 1.3 μm. Elevated temperature crystallization results in less-well distributed porosity and larger detonation failure thicknesses. Despite these differences in critical thickness, detonation velocity in thick films is consistent and thus we believe that only the microstructure and not the density of the films is significantly affected by different crystallization conditions. Future work

will comprise of continuing to develop relationships between sample preparation, microstructure, and detonation properties towards improving our understanding of the effects of microstructure on detonation.

Acknowledgements

The authors wish to acknowledge Michael P. Marquez, James Patrick Ball, Jill C. Miller, and M. Barry Ritchey for experimental support. Adrian L. Casias, Adrian Wagner, and Benjamin J. Hanks assisted with manufacturing deposition and testing hardware. The Joint Department of Defense/Department of Energy Munitions Technology Development Program supported this work. Sandia National Laboratories is a multi-program laboratory managed and operated by Sandia Corporation, a wholly owned subsidiary of Lockheed Martin Corporation, for the U.S. Department of Energy's National Nuclear Security Administration under contract DE-AC04-94AL85000.

References

1. Kotomin, A., Kozlov, A., and Dushenok, S., "Detonatability of High-Energy-Density Heterocyclic Compounds," *Russian Journal of Physical Chemistry B, Focus on Physics*, vol. 1, pp. 573-575, 2007.
2. Petel, O.E., Mack, D., Higgins, A.J., Turcotte, R., and Chan, S.K., "Minimum propagation diameter and thickness of high explosives," *Journal of Loss Prevention in the Process Industries*, vol. 20, pp. 578-583, 2007.
3. Baer, M.R., Kipp, M.E., and van Swol, F., "Micromechanical Modeling of Heterogeneous Energetic Materials," *Eleventh International Detonation Symposium* Snowmass, CO, August 30-September 4, 1998, pp. 788-797.
4. Tappan, A.S., Knepper, R., Wixom, R.R., Marquez, M.P., Miller, J.C., and Ball, J.P., "Critical Thickness Measurements in Vapor-Deposited Pentaerythritol Tetranitrate (PETN) Films," *14th International Detonation Symposium*, Coeur d'Alene, ID, April 11 – 16, 2010, pp. 1087 – 1095.
5. Tappan, A.S., Knepper, R., Wixom, R.R., Marquez, M.P., Ball, J.P., and Miller, J.C., "Critical Detonation Thickness in Vapor-Deposited Pentaerythritol Tetranitrate (PETN) Films," *17th APS Topical Conference on Shock Compression of Condensed Matter*, Chicago, IL, June 26 – July 1, 2011.
6. Knepper, R., Marquez, M.P., and Tappan, A.S., "Effects of Confinement on Detonation Behavior of Vapor-Deposited Hexanitroazobenzene Films," *15th International Detonation Symposium*, San Francisco, CA, July 13-18, 2014.
7. Knepper, R., Browning, K., Wixom, R.R., Tappan, A.S., Rodriguez, M.A., and Alam, M.K., "Microstructure Evolution during Crystallization of Vapor-Deposited Hexanitroazobenzene Films," *Propellants, Explosives, Pyrotechnics*, vol. 37, pp. 459 – 467, 2012.
8. Wixom, R.R., Tappan, A.S., Brundage, A.L., Knepper, R., Ritchey, M.B., Michael, J.R., and Rye, M.J., "Characterization of pore morphology in molecular crystal explosives by focused ion-beam nanotomography," *Journal of Materials Research*, vol. 25, pp. 1362-1370, July 1, 2010.
9. Campbell, A.W. and Engelke, R., "The Diameter Effect in High-Density Heterogeneous Explosives," *6th Symposium (International) on Detonation*, Coronado, CA, August 24-27, 1976, pp. 642-652.